JACS
JOURNAL OF THE AMERICAN CHEMICAL SOCIETY

Communication

pubs.acs.org/JACS

Nontemplate Synthesis of $CH_3NH_3PbBr_3$ Perovskite Nanoparticles

Luciana C. Schmidt,[†,§] Antonio Pertegás,[†] Soranyel González-Carrero,[†] Olga Malinkiewicz,[†] Said Agouram,[‡] Guillermo Mínguez Espallargas,[†] Henk J. Bolink,[†] Raquel E. Galian,*[,†] and Julia Pérez-Prieto*[,†]

[†]Instituto de Ciencia Molecular (ICMol), Universidad de Valencia, Catedrático José Beltrán 2, 46980 Paterna, Valencia, Spain

[‡]Department of Applied Physics and Electromagnetism, University of Valencia, Edif. Investigación, c/Dr. Moliner 50, 46100 Burjassot, Spain

Supporting Information

ABSTRACT: To date, there is no example in the literature of free, nanometer-sized, organolead halide $CH_3NH_3PbBr_3$ perovskites. We report here the preparation of 6 nm-sized nanoparticles of this type by a simple and fast method based on the use of an ammonium bromide with a medium-sized chain that keeps the nanoparticles dispersed in a wide range of organic solvents. These nanoparticles can be maintained stable in the solid state as well as in concentrated solutions for more than three months, without requiring a mesoporous material. This makes it possible to prepare homogeneous thin films of these nanoparticles by spin-coating on a quartz substrate. Both the colloidal solution and the thin film emit light within a narrow bandwidth of the visible spectrum and with a high quantum yield (ca. 20%); this could be advantageous in the design of optoelectronic devices.

Organic−inorganic hybrid materials combine useful properties of both organic and inorganic materials, such as plastic mechanical properties (organic material) and good electronic mobility (inorganic material).[1] Among this type of materials, there is presently a great interest in organolead halide perovskites of general $APbX_3$ (A = organic ammonium cation, X = halide anion) stoichiometry. In these compounds, the lead cations are in a 6-fold coordination and are surrounded by an octahedron of halide anions together with the ammonium cations in a 12-fold cuboctahedral coordination.[1,2] These perovskites are versatile materials prepared from abundant and low cost starting compounds and exhibit very interesting features, such as unique optical[3] and excitonic properties,[4] as well as electrical conductivity.[5]

Specifically, the iodide and bromide versions of $CH_3NH_3PbX_3$ have led to a breakthrough performance in thin film solar cells.[3,5−7]

First reports of the use of these perovskites in photovoltaic applications were obtained with solar cells employing mesoporous metal oxides, such as titania[3−5,7,8] and alumina,[6,8−10] whose porosity permits the formation of $CH_3NH_3PbX_3$ perovskite nanoparticulate material, i.e., the confinement of the array extending in three dimensions to the nanometer scale to build zero-dimensional material. Optimization of the device, specifically filling the pores with the perovskites, has led to very highly efficient devices as was recently reported by the Grätzel group.[3] It has also been demonstrated that a thin film of bulk $CH_3NH_3PbX_3$ deposited on top of an n-type metal oxide leads to solar cells with efficiencies around 10.9%.[10] This is particularly interesting as it indicates that the perovskite layer (the thickness was around 300 nm) not only functions as the principal light absorber[11] but also as the transporter of electrons and/or holes.[12] Hence, $CH_3NH_3PbX_3$ perovskites, both as confined nanomaterials in nanoporous materials,[3−12] and as "bulk" thin films, have led to efficient solar cells. Thin films prepared with $APbX_3$ perovskite nanoparticles could outperform the above-mentioned architectures, but no suitable synthetic procedure to obtain particles with sizes as small as several nanometers has yet been reported.

The availability of stable colloidal solutions of $CH_3NH_3PbX_3$ nanoparticles and mainly those with sizes below 10 nm would enable the preparation of new device architectures that could further enhance solar cell performance and elucidate perovskite operational mechanisms. Such colloidal solutions of nanometer-sized $APbX_3$ perovskites have, to our knowledge, not been reported. We presumed that by following the strategies described for the synthesis of quantum dots (zero-dimensional materials), a good organic capping agent, such as long alkyl chain amines, would favor the formation of $CH_3NH_3PbX_3$ nanoparticles, which would eventually be dispersible in aprotic solvents.[13−15]

In this report, we demonstrate the preparation of highly crystalline 6 nm-sized $CH_3NH_3PbX_3$ nanoparticles as stable colloidal solutions. Highly fluorescent thin films and first electroluminescent devices were prepared using the colloidal solution of these nanoparticles.

The perovskite nanoparticles were prepared using bromide, rather than iodide, due to the higher stability of the former,[16] and due to the most interesting luminescent properties. The nanoparticles were synthesized using a simple and reliable preparation method in which a mixture of CH_3NH_3Br and a medium or long chain alkyl ammonium bromide was reacted with $PbBr_2$ in the presence of oleic acid and octadecene. We propose that while the methyl ammonium cations are embedded in the voids of a set of corner-sharing PbX_6 octahedra (Figure 1), the longer alkyl chain cations only fit the periphery of the octahedra set with their chains dangling

Received: October 31, 2013
Published: January 3, 2014

   dx.doi.org/10.1021/ja4109209 | J. Am. Chem. Soc. 2014, 136, 850−853

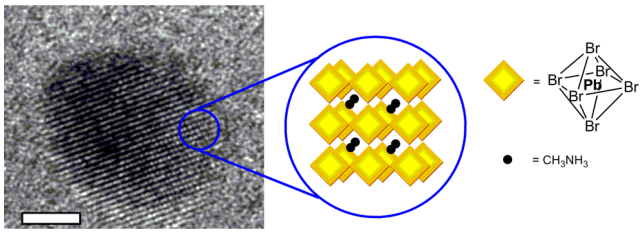

Figure 1. HRTEM image of an isolated perovskite nanoparticle (scale bar 2 nm) and schematic representation of an array of corner sharing MX_6 octahedra confined in the three dimensions due to the organic capping.

outside it. Thus, these ammonium ions would act as the capping ligands of the nanoparticle, limiting the growth of the array extending in three dimensions. This strategy produces intrinsic perovskite nanoparticles stabilized by the alkyl chains.

To prove the preparation of the $CH_3NH_3PbX_3$ perovskite nanoparticles was achievable, besides adding methylammonium bromide (CH_3NH_3Br), the long alkyl chain ammonium cation octylammonium bromide or octadecylammonium bromide was used in the preparation of the material. This longer chain alkyl ammonium cation might act as a better capping ligand to isolate the nanoparticle core, while nanoparticles with the methylammonium cation might be advantageous in the application of the nanoparticles in solar cells.[17]

In all the cases, the addition of the long chain ammonium bromide to a warm (80 °C) solution of oleic acid in octadecene (a noncoordinating solvent), was followed by the consecutive addition of methylammonium bromide and $PbBr_2$, and right after, addition of acetone induced the precipitation of a yellow solid from the solution. The methylammonium salt and the lead bromide had previously been dissolved in a small amount of dimethylformamide (DMF) to improve their solubility in the media. The total ammonium salt concentration was kept at 0.045 M and a $PbBr_2$ equimolar concentration was used. Remarkably, the solid proved to be dispersible in toluene, thus suggesting the formation of perovskite nanohybrids. For comparisons sake, the reaction between the CH_3NH_3Br and the lead bromide under the same conditions led to an orange solid that could hardly be dispersed in toluene.

To determine the best molar ratio between the ammonium salts, preliminary assays were carried out using octadecylammonium bromide. The $CH_3(CH_2)_{17}NH_3Br/CH_3NH_3Br$ molar ratios used were 0.5:0.5, 0.6:0.4, and 0.7:0.3 and the samples were labeled as $P_{ODA}1$, $P_{ODA}2$, and $P_{ODA}3$, respectively, in which P refers to perovskite, ODA refers to octadecylammonium cation, and 1,2,3 indicates an increasing molar ratio.

The UV−visible absorption spectra of the colloidal solutions exhibit a peak at ca. 525 nm, 16 nm blue-shifted compared to that of $CH_3NH_3PbBr_3$ bulk that can be attributed mainly to the particle-size quantum confinement effect in the $APbBr_3$ nanoparticles (Figures S1A, S2A, and S3A for $P_{ODA}1$, $P_{ODA}2$, and $P_{ODA}3$, respectively); a similar absorption has been reported for $CH_3NH_3PbBr_3$ within mesoporous titania and alumina.[6] Consequently, the long chain ammonium salt played a key role in the formation of the hybrid perovskite nanoparticles and in their capacity to give rise to colloidal solutions.

However, in addition to the peak at ca. 525 nm, the spectra of the P_{ODA} samples presented others at lower wavelengths, suggesting that the formation of the $APbBr_3$ perovskite structure was accompanied by the formation of perovskites with other stoichiometries.[18−21] Transmission electron microscopy (TEM) images showed that the $CH_3(CH_2)_{17}NH_3Br/CH_3NH_3Br$ 0.6:0.4 molar ratio used in $P_{ODA}2$ proved to be the most effective in the formation of nanoparticles (see Figures S4, S5, and S6 for $P_{ODA}1$, $P_{ODA}2$, $P_{ODA}3$, respectively). Interestingly, the fluorescence spectra of the P_{ODA} samples mainly showed the near band edge emission attributable to the $APbBr_3$ nanoparticles with a narrow full width at the half-maximum (fwhm). The emission wavelength maximum and fwhm values were at 529 (fwhm = 26 nm), at 526 (fwhm = 24 nm), and at 524 nm (fwhm = 23 nm) for $P_{ODA}1$, $P_{ODA}2$, and $P_{ODA}3$, respectively. However, while this emission band was highly symmetrical in the case of $P_{ODA}2$ and $P_{ODA}3$, this was not the case for $P_{ODA}1$, which showed a shape similar to that of $CH_3NH_3PbBr_3$ bulk (Figures S1B, S2B, and S3B).

The rather long chain of ODA might make the formation of perovskites with other stoichiometries competitive with the formation of the $CH_3NH_3PbX_3$ nanoparticles. Therefore, assays were performed using the shorter octylammonium bromide ($CH_3(CH_2)_7NH_3Br$) in the synthesis of the nanoparticles. In addition, as mentioned above, the use of shorter alkyl ammonium cations could be advantageous for future applications of these nanoparticles. The $CH_3(CH_2)_7NH_3Br/CH_3NH_3Br$ 0.6:0.4 molar ratio was used since it seemed to be the best ratio for the preparation of the $CH_3NH_3PbX_3$ nanoparticles, taking into account the full set of data (resulting from TEM, absorption, and emission measurements) for P_{ODA}.

Remarkably, $P_{OA}2$ (OA refers to octylammonium cation) also proved to be dispersible in toluene and its absorption spectrum exhibited a peak at λ_{max} 527 nm (Figure 2a).

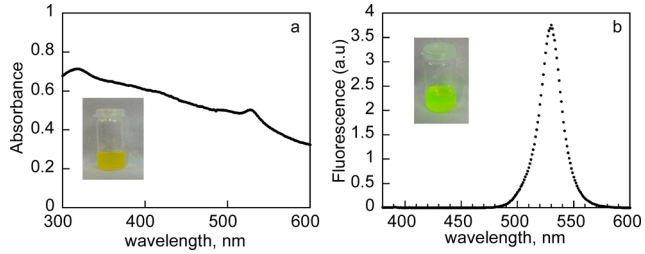

Figure 2. UV−visible absorption (a) and room-temperature fluorescence (b) spectra of $P_{OA}2$ in toluene. Inset: photographs of the emitter illuminated with ambient light (a) and UV light-lamp centered at 365 nm (b).

Even more remarkably, its emission spectrum only exhibited a highly symmetric band centered at λ_{max} = 530 nm, which was narrower (fwhm = 21 nm) than that of the P_{ODA} samples (Figure 2b). The very small Stokes shift indicates that the structure does not undergo changes when it is in the excited state and that it is a rigid structure. Hence, considerable autoabsorption occurs which hinders the determination of the exact photoluminescence quantum yield (Φ_f) and a value of 17% was registered when using considerably diluted solutions and the excitation wavelength was as far away as possible from the absorption maximum. It has been reported that excitons in the bulk $CH_3NH_3PbBr_3$ are of the Wannier type, producing a strong delocalization due to the weak exciton binding energy of 0.076 eV.[22] Therefore, the high Φ_f for the colloidal dispersions indicates that the exciton binding energy is significantly increased, preventing dissociation of the exciton prior to its radiative decay.

dx.doi.org/10.1021/ja4109209 | J. Am. Chem. Soc. 2014, 136, 850−853

All these data suggested that the preparation of $APbBr_3$ perovskite nanoparticles had been successful when using OA as the capping ligand and a 0.6:0.4 $CH_3(CH_2)_7NH_3Br$/CH_3NH_3Br molar ratio. It is worth mentioning that the fluorescence of the $P_{OA}2$ was higher than the $P_{ODA}2$ (Figure S7). In addition, these results indicated that the length of the alkyl chain of the ammonium cation exerted a considerable effect; thus, the composition homogeneity in $APbBr_3$ nanoparticles was greater for $P_{OA}2$ samples, with an alkyl chain of eight carbon atoms, than that of $P_{ODA}2$ with 18 carbon atoms.

Remarkably, $P_{OA}2$ samples showed an extraordinary stability under light illumination (see Figure S8, irradiation under two different conditions).

To probe the dispersibility of P_{OA2} (2 mg/mL), the following organic solvents were used: toluene, hexane, tetrahydrofuran, chloroform, dioxane, dimethylsulfoxide, anisole, ethyl acetate, isopropanol, and methanol. $P_{OA}2$ formed stable colloidal solution in all the solvents except in DMSO and isopropanol, where the solution became immediately colorless. This suggested that the nanoparticles reverted back to their precursors in the highly polar aprotic solvent as well as in the protic solvents (Figure S9).

The X-ray powder diffraction (XRPD) pattern of the solid sample of $P_{OA}2$ was measured to further confirm the phase purity of $P_{OA}2$ as well as the crystallinity of the sample (Figure S10). The XRPD pattern of the sample showed that it was highly crystalline. Pawley refinement[23,24] performed by using the TOPAS computer program, demonstrated that $P_{OA}2$ presented an excellent fit to a single-phase model corresponding to the cubic phase of the hybrid organic−inorganic $CH_3NH_3PbBr_3$ perovskite (a = 5.9334 (5) Å, space group = Pm-3m).[25,26] The list of peak positions of the XRPD pattern is shown in Table S1. Energy-dispersive X-ray spectroscopy (EDS) analysis in nanoprobe mode showed that $P_{OA}2$ presented a Br/Pb ratio of 77/23 in good agreement with a $PbBr_3$ stoichiometry. In addition, TEM images of $P_{OA}2$ sample proved it mainly consisted of spherical nanoparticles with an average size of 6.2 ± 1.1 nm (Figure S11).

Figure 3 shows representative high resolution TEM (HRTEM) images of one nanoparticle and their corresponding fast Fourier transform (FFT) patterns, indicating that the nanoparticles possess crystalline surfaces with no sign of an amorphous layer. The HRTEM images show well-defined lattice spacing and FFT patterns and well-defined spots which are in accordance with the crystallographic parameters for the $CH_3NH_3PbBr_3$ bulk, thus demonstrating not only that the nanoparticles were highly crystalline but also that they possessed the same stoichiometry as the bulk. The images in Figure 3 show an interplanar distance from fringes of about 2.98 Å, which is characteristic of (002) planes of cubic phase structure of $CH_3NH_3PbBr_3$ with Pm-3m space group, two interplanar spacing measurements at about 2.103 and 1.87 Å, which can be attributed to (022) and (031) family planes, respectively, and are in good agreement with the data for a cubic structure with lattice parameter of about 5.93 Å. The mean value of a-lattice parameter determined from d-spacing of 5.95 ± 0.03 Å was in good agreement with the XRPD value of 5.9334 (5) Å measured in the bulk perosvkite

The crystalline $P_{OA}2$ nanoparticles kept in the solid state for more than three months proved to be dispersible in toluene. The colloidal solutions were stable for up to 24 h. Consequently, in a first attempt to make use of the colloidal dispersion of $P_{OA}2$ as a starting material for optoelectronic

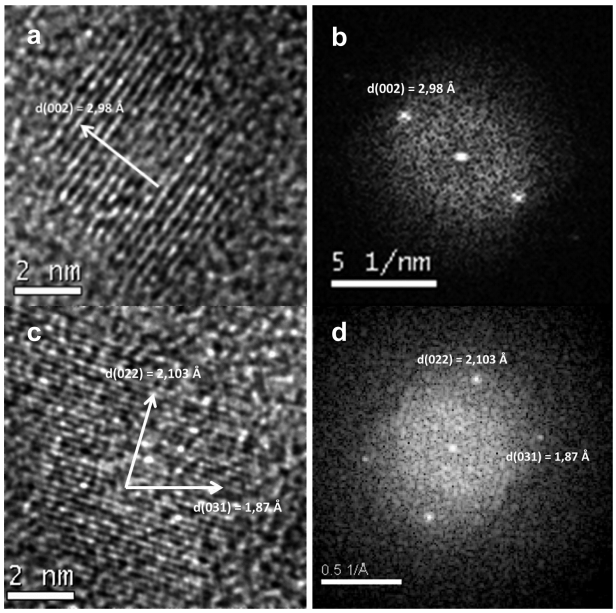

Figure 3. HRTEM images of individual nanoparticles from $P_{OA}2$ (a and c) and their corresponding FFT analyses (b and d).

devices, such solutions were used to prepare a homogeneous and fluorescent thin film on a quartz substrate. Thin films were prepared simply by spin-coating the colloidal solution on a thoroughly cleaned substrate. To facilitate good adhesion of the nanoparticles a short O_2 plasma treatment was employed to ensure a polar top surface of the substrates.

The emission spectrum of $P_{OA}2$ film also showed a narrow emission band (fwhm = 22 nm) whose maximum was at 533 nm, i.e., only 3 nm red-shifted compared to that of $P_{OA}2$ colloidal solution in toluene (Figure 4). The Φ_f of the film,

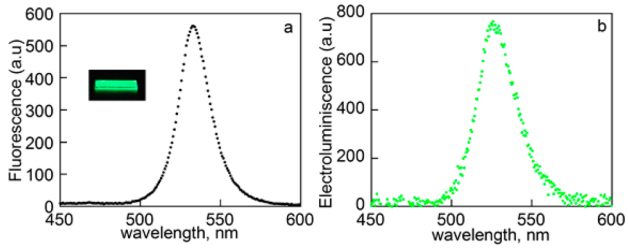

Figure 4. (a) Room-temperature fluorescence spectrum (λ_{exc} = 350 nm) of a thin film prepared using colloidal $P_{OA}2$. (b) Room-temperature electroluminescent spectrum of the device ITO/PEDOT:PSS/pTPD/$P_{OA}2$/Ba/Ag at 6 V.

measured with an integration sphere, was ca. 23%. As mentioned previously, there is a considerable amount of autoabsorption due to the very small Stokes shift in the nanoparticles. Therefore, for these films, in which the nanoparticles are present at high concentration, the Φ_f is less accurate and the registered value is most likely to be at a higher level as part of the emitted light is reabsorbed by the particles, thus leading to radiative losses.

A thin film light-emitting device based on $P_{OA}2$ nanoparticles was also prepared and its performance was compared with that of a reference device based on a bulk film of the same material (Figure S12). A very strong improvement in the electroluminescence is observed when the nanoparticles are used. This

dx.doi.org/10.1021/ja4109209 | J. Am. Chem. Soc. 2014, 136, 850−853

clearly demonstrates the benefit of nanoparticles over bulk films in already one application.

We also succeeded to prepare $APbI_3$ nanoparticles by performing small variations on the here reported strategy; the preliminary results are promising (Figure S13), but a better homogeneity of the samples is expected by further fine-tuning of the preparation method for these systems.

In summary, our results show that hybrid organic−inorganic $APbBr_3$ (A: alkyl ammonium ion) perovskite nanoparticles can be easily and efficiently prepared. The method makes use of the capacity of medium alkyl chain organic ammonium cations to stabilize small sized (ca. 6 nm) crystalline nanoparticles. These nanoparticles can be kept stable in a solid state and maintained dispersed in aprotic, moderate polarity, organic solvents for more than three months. This made the preparation of a homogeneous thin film by spin-coating on a quartz substrate at room temperature possible. This fact is promising, since perovskite films could be compatible with flexible substrates. Both the colloidal solution and the film exhibit a high Φ_f and a narrow emission band, whose λ_{max} only changed slightly from the colloidal solution to the film, although considerably blue-shifted compared to that of the $CH_3NH_3PbBr_3$ bulk perovskite. Studies on the suitability of other combinations of short/long chain ammonium salts for preparing stable hybrid $PbBr_3$ colloidal solutions (for their application in optical devices) is worth studying and will be performed in due course.

■ ASSOCIATED CONTENT

Supporting Information

Spectroscopy data and TEM images of the perovskite nanoparticles. This material is available free of charge via the Internet at http://pubs.acs.org.

■ AUTHOR INFORMATION

Corresponding Authors

raquel.galian@uv.es

julia.perez@uv.es

Present Address

[§]L.C.S.: CONICET-INFIQC, Dpto. Qca. Org., UNC, Haya de la Torre y Medina Allende, Ciudad Univ., 5000-Córdoba, Argentina

Notes

The authors declare no competing financial interest.

■ ACKNOWLEDGMENTS

We thank the Spanish Ministry of Economy and Competitiveness (MINECO Project CTQ2011-27758, MAT2011-24594 and FPI grant to A.P.), European Community (Seventh Framework Programme, ORION, Grant 229036), Generalitat Valenciana (Prometeo/2012/053, ACOMP/2013/008, and FGUV (H.J.B. and R.E.G.)). The authors are grateful to SCSIE, University of Valencia for providing HRTEM facility. This article is dedicated to Professor Gregorio Asensio on the occasion of his 65th birthday.

■ REFERENCES

(1) Mitzi, D. B. In *Progress in Inorganic Chemistry*; John Wiley & Sons, Inc.: New York, 1999; Vol. *48*, p 1.

(2) Mitzi, D. B. *J. Chem. Soc., Dalton Trans.* **2001**, 1.

(3) Burschka, J.; Pellet, N.; Moon, S.-J.; Humphry-Baker, R.; Gao, P.; Nazeeruddin, M. K.; Grätzel, M. *Nature* **2013**, *499*, 316.

(4) Cai, B.; Xing, Y.; Yang, Z.; Zhang, W.-H.; Qiu, J. *Energy Environ. Sci.* **2013**, *6*, 1480.

(5) Kim, H.-S.; Lee, C.-R.; Im, J.-H.; Lee, K.-B.; Moehl, T.; Marchioro, A.; Moon, S.-J.; Humphry-Baker, R.; Yum, J.-H.; Moser, J. E.; Grätzel, M.; Park, N.-G. *Sci. Rep.* **2012**, *2*, 591.

(6) Kojima, A.; Ikegami, M.; Teshima, K.; Miyasaka, T. *Chem. Lett.* **2012**, *41*, 397.

(7) Kojima, A.; Teshima, K.; Shirai, Y.; Miyasaka, T. *J. Am. Chem. Soc.* **2009**, *131*, 6050.

(8) Noh, J. H.; Im, S. H.; Heo, J. H.; Mandal, T. N.; Seok, S. I. *Nano Lett.* **2013**, *13*, 1764.

(9) Carnie, M. J.; Charbonneau, C.; Davies, M. L.; Troughton, J.; Watson, T. M.; Wojciechowski, K.; Snaith, H.; Worsley, D. A. *Chem. Commun.* **2013**, *49*, 7893.

(10) Lee, M. M.; Teuscher, J.; Miyasaka, T.; Murakami, T. N.; Snaith, H. J. *Science* **2012**, *338*, 643.

(11) Ball, J. M.; Lee, M. M.; Hey, A.; Snaith, H. J. *Energy Environ. Sci.* **2013**, *6*, 1739.

(12) Etgar, L.; Gao, P.; Xue, Z.; Peng, Q.; Chandiran, A. K.; Liu, B.; Nazeeruddin, M. K.; Grätzel, M. *J. Am. Chem. Soc.* **2012**, *134*, 17396.

(13) Talapin, D. V.; Rogach, A. L.; Kornowski, A.; Haase, M.; Weller, H. *Nano Lett.* **2001**, *1*, 207.

(14) Wadhavane, P. D.; Galian, R. E.; Izquierdo, M. A.; Aguilera-Sigalat, J.; Galindo, F.; Schmidt, L.; Burguete, M. I.; Pérez-Prieto, J.; Luis, S. V. *J. Am. Chem. Soc.* **2012**, *134*, 20554.

(15) Aguilera-Sigalat, J.; Rocton, S.; Sanchez-Royo, J. F.; Galian, R. E.; Perez-Prieto, J. *RSC Adv.* **2012**, *2*, 1632.

(16) Baikie, T.; Fang, Y.; Kadro, J. M.; Schreyer, M.; Wei, F.; Mhaisalkar, S. G.; Grätzel, M.; White, T. J. *J. Mater. Chem. A* **2013**, *1*, 5628.

(17) Sun, L.; Choi, J. J.; Stachnik, D.; Bartnik, A. C.; Hyun, B.-R.; Malliaras, G. G.; Hanrath, T.; Wise, F. W. *Nat. Nanotechnol.* **2012**, *7*, 369.

(18) Tabuchi, Y.; Asai, K.; Rikukawa, M.; Sanui, K.; Ishigure, K. *J. Phys. Chem. Solids* **2000**, *61*, 837.

(19) Takeoka, Y.; Fukasawa, M.; Matsui, T.; Kikuchi, K.; Rikukawa, M.; Sanui, K. *Chem. Commun.* **2005**, 378.

(20) Audebert, P.; Clavier, G.; Alain-Rizzo, V. R.; Deleporte, E.; Zhang, S.; Lauret, J.-S. B.; Lanty, G. T.; Boissière, C. D. *Chem. Mater.* **2009**, *21*, 210.

(21) Vincent, B. R.; Robertson, K. N.; Cameron, T. S.; Knop, O. *Can. J. Chem.* **1987**, *65*, 1042.

(22) Tanaka, K.; Takahashi, T.; Ban, T.; Kondo, T.; Uchida, K.; Miura, N. *Solid State Commun.* **2003**, *127*, 619.

(23) Pawley, G. *J. Appl. Crystallogr.* **1981**, *14*, 357.

(24) Coelho, A. A.; *TOPAS-Academic*, 4.1 ed.; Coelho Software: Brisbane, Australia, 2007.

(25) Knop, O.; Wasylishen, R. E.; White, M. A.; Cameron, T. S.; Oort, M. J. M. V. *Can. J. Chem.* **1990**, *68*, 412.

(26) Poglitsch, A.; Weber, D. *J. Chem. Phys.* **1987**, *87*, 6373.